Nanomedicine: Interaction of biomimetic apatite colloidal nanoparticles with human blood components

Maëla Choimet[a,1], Hyoung-Mi Kim[b,1], Jae-Min Oh[b,**], Audrey Tourrette[a], Christophe Drouet[a,*]

[a] CIRIMAT, Universite de Toulouse, CNRS, INPT, UPS, Ensiacet, Toulouse, France
[b] Nano Bio Materials Laboratory, Dept. Chemistry and Medical Chemistry, Yonsei University, Wonju, South Korea

ARTICLE INFO

Keywords:
Apatite nanoparticles
Hemolysis
Protein fluorescence quenching
Blood cells
Hemocompatibility

ABSTRACT

This contribution investigates the interaction of two types of biomimetic-apatite colloidal nanoparticles (negatively-charged 47 nm, and positively-charged 190 nm NPs) with blood components, namely red blood cells (RBC) and plasma proteins, with the view to inspect their hemocompatibility. The NPs, preliminarily characterized by XRD, FTIR and DLS, showed low hemolysis ratio (typically lower than 5%) illustrating the high compatibility of such NPs with respect to RBC, even at high concentration (up to 10 mg/ml). The presence of glucose as water-soluble matrix for freeze-dried and re-dispersed colloids led to slightly increased hemolysis as compared to glucose-free formulations. NPs/plasma protein interaction was then followed, via non-specific protein fluorescence quenching assays, by contact with whole human blood plasma. The amount of plasma proteins in interaction with the NPs was evaluated experimentally, and the data were fitted with the Hill plot and Stern-Volmer models. In all cases, binding constants of the order of 10^1–10^2 were found. These values, significantly lower than those reported for other types of nanoparticles or molecular interactions, illustrate the fairly inert character of these colloidal NPs with respect to plasma proteins, which is desirable for circulating injectable suspensions. Results were discussed in relation with particle surface charge and mean particle hydrodynamic diameter (HD). On the basis of these hemocompatibility data, this study significantly complements previous results relative to the development and nontoxicity of biomimetic-apatite-based colloids stabilized by non-drug biocompatible organic molecules, intended for use in nanomedicine.

1. Introduction

In recent years, a considerable literature has grown up around the theme of materials in the area of nanomedicine, as drug nanocarriers or as nanoprobe for imaging [1–11]. This research field led to increasing interest in the study of the behavior of nanoparticles (NPs) intended for systemic circulation, including in terms of hemocompatibility. Indeed, after administration in vivo, NPs biodistribution to the immune cells and organs can be affected by interaction with the immune system of the patient. According to Dobrovolskaia et al. [12], some factors have to be taken into account to evaluate this process. Biodistribution comprehension and biocompatibility evaluation then requires several investigations, including in particular the study of the possible interaction of the NPs with blood components, namely red blood cells (erythrocyte, or "RBC") – comprising hemolysis assays – and plasma proteins. In this view, various publications report particle interactions with RBC [13–17], underlining the role of particle size and surface state. Research results dealing with hemocompatibility moreover tend to point out the strong influence of NPs size [18], surface charge [19] and overall surface properties [14].

In the search for appropriate and potentially multifunctional systems for nanomedicine, bio-inspired systems appear particularly appealing due to their expectedly high intrinsic biocompatibility. In this context, apatite-based systems – approaching the mineral part of bones – represent in particular a promising type of biocompatible systems; and previous works have shown the possibility to obtain colloidal-like formulations of apatite nanoparticles through surface engineering [1,20–23]. Apatite-based NPs may thus be considered as promising potential candidates for

* Corresponding author at: CIRIMAT-Ensiacet, 4 all. Emile Monso, 31030 Toulouse cedex 4, France.
** Corresponding author at: 1 Yonseidaegil, Wonju, Gangwon, Republic of Korea (South Korea)
E-mail addresses: jaemin.oh@yonsei.ac.kr (O. Jae-Min), christophe.drouet@ensiacet.fr (C. Drouet).
[1] These authors equally contributed to this work.

http://dx.doi.org/10.1016/j.colsurfb.2016.04.038

use in nanomedicine. Whether surface-covered with heparin, polyethyleneimine, or uncovered, a few previous literature works studied the blood compatibility of nanosized apatitic compositions exhibiting different surface properties, or of apatite-coated magnetite NPs, in view of different kinds of applications such as drug delivery [19,24,25] or for the fabrication of nano-contrast agents for in vivo imaging [26]. In all cases, these apatitic or apatite-coated NPs were not found to cause hemolysis (<5%) in the conditions tested. Some other aspects also conveyed elements informing on the high biocompatibility of apatitic or apatite-coated NPs, based on the exploration of platelet activation [26], cytotoxicity [6,26,27], in vivo acute toxicity [25], or else non pro-inflammatory potential [6]. Inspecting the behavior of (nano)particles with blood components also includes the study of their interaction with plasma proteins. Montazeri et al. [28] showed that proteins could interact with fluoride-substituted apatite powders, in a way dependent on fluoride content which may be optimized to improve biological response. Lacerda et al. reported that gold NPs showed different types of protein interaction according to their size and to the type of proteins [17].

Taking into account the promise of apatite nanosystems in medicine, the confirmation of their high biocompatibility on an experimental basis therefore remains one key point, explaining the increasing interest shown by the scientific/medical communities as highlighted above.

In particular, the interaction of dispersed apatite NPs with plasma proteins has only seldom been explored, which is one of the objectives of the present contribution. Also, apatite particles easily agglomerate; consequently, formulations intended for administrations through injections (whether intravenous or intratumoral for example) need be stabilized as colloidal-like suspensions: this can be achieved through surface modification via an organic corona. To be envisioned for use in the human body, this corona should also be composed of biocompatible constituting molecules. In our approach initiated several years ago [1,22,29], this stabilization is for example realized by surface grafting of either a phospholipid moiety (2-aminoethylphosphate, or AEP, representing hydrophilic head of the phospholipid phosphatidylethanolamine, a component of cell membranes) [30] or a phosphonate-terminated polyethyleneglycol (denoted (PEG)P). Obtained stabilized apatite colloidal nanoparticles, involving a biomimetic apatite phase close to bone mineral (nonstoichiometric apatite with surface active sites) [31] and stabilized with AEP, were for example shown to exhibit high cytocompatibility towards different types of cells (mesenchymal stem cells form adipose tissue, breast cancer cells), and no pro-inflammatory potential was detected when these NPs were contacted with human monocytes/macrophages [6]. In the present work, in addition to following the interaction of human blood plasma proteins with both AEP- and (PEG)P-stabilized biomimetic apatite NPs, the contact with red blood cells was also explored through hemolysis assays for complementing their hemocompatibility evaluation.

2. Materials and methods

2.1. Synthesis of colloidal apatite NPs

Colloidal formulations were performed as described in a previous work [21,22]. Briefly, the precipitation of biomimetic nanocrystalline apatite was carried out in deionised water, at room temperature and pH 9.5. After the mixing of a solution of calcium nitrate (1.15 g in 18.75 ml) and dispersing agent (AEP: 0.687 g or (PEG)P: 0.396 g) and a solution of di-ammonium hydrogen phosphate (0.21 g in 6.25 ml), the pH was adjusted to 9.5, by addition of ammonia. The suspension was then placed in an oven preset at 100 °C in a sealed vial for maturation of 16 h. In this study, two types of colloids, with different stabilizing agents, were investigated: AEP, acting as an electrostatic stabilizing agent, and (PEG)P acting by steric hindrance (MW: 5200 g/mol). Both types of colloids obtained were then purified by dialysis to remove unattached dispersing agent and any unreacted reagents, at room temperature, with membranes of different Molecular Weight Cut-Off (MWCO), respectively 6000–8000 and 12,000–14,000 MCWO for AEP and (PEG)P colloids. The dialysis process, used to remove unreacted species, is detailed elsewhere [32]. For AEP samples, an increase of suspension viscosity may occur during dialysis. The addition of sodium hexametaphosphate (denoted HMP) to this sample then allowed obtaining well dispersed AEP-stabilized nanoparticles, as well as a pH close to neutral. The final pH of each colloid was finally adjusted to the physiological value, which was undergone on (PEG)P colloids by addition of HCl 0.37%. To study NPs interactions with human blood components, some colloids were used directly in the suspension state, and some others were lyophilized and re-dispersed at the time of use. Prior to lyophilization, glucose was added to each sample (0.066 M) to keep colloidal properties with unchanged particle HD after re-dispersion [23]. Each colloid was then prepared to have a final NaCl concentration of 0.9 w/v%. The notation “AN” and “AG” correspond to AEP-stabilized colloids respectively in suspension (with NaCl) and in lyophilized form (with glucose and NaCl). Similarly, for (PEG)-P-stabilized colloids, the notations “PN” and “PG” will be used.

When mentioned in the text, a non-colloidal reference sample was also prepared by following the same protocol as above but in the absence of stabilizing agent.

2.2. Physico-chemical characterization of apatite colloidal NPs

The structure of the calcium phosphate nanoparticles contained in freeze-dried suspensions was characterized by powder X-ray diffraction using an Equinox 1000 curved-counter INEL diffractometer (acquisition time 2 h) with a cobalt anticathode (λ_{Co} = 1.78892 Å). Fourier transform infrared (FTIR) spectroscopy analyses were performed on a Thermo-Nicolet 5700 spectrometer with a resolution of 4 cm^{-1}, in the wavenumber range of 400–4000 cm^{-1}, using the KBr pellet method. Particle HD (determined by dynamic light scattering, DLS) was measured on a Nanosizer ZS apparatus (Malvern Instruments, λ = 630 nm). In order to evaluate surface charge of NPs, suspension or powder NPs were diluted or dispersed in deionized water at an appropriate range of concentration (1 ∼ 1.8 mg/ml) and subjected to zeta potential measurement utilizing Otsuka ELS-Z 1000 instrument. Zeta potential and hydrodynamic diameter of each apatite sample were also evaluated after treatment in human plasma. Plasma obtained from human whole blood (approved by the Yonsei University Wonju College of Medicine (Approval No. YWMR-12-6-030)) was diluted 50 times with Dulbecco's phosphate buffered saline (DPBS) and mixed with 0.25 mg/ml (for zeta potential) and 1 mg/ml (for DLS) of apatite sample in 1:1 volume ratio.

2.3. Hemolysis assays

Hemolysis assay allowed evaluating the toxicity of our colloids on red blood cells (RBC) by following the possible release of hemoglobin upon contact with the NPs. The procedure used was inspired from other studies [33–35]. For these tests, whole human blood samples were freshly obtained from a healthy volunteer and directly used for the assay. These experiments utilizing human whole blood were approved by the Yonsei University Wonju College of Medicine (Approval No. YWMR-12-6-030). Deionized water and saline were added to RBC suspension, as the positive and negative controls, respectively.

First, colloidal NPs were suspended in saline in different concentrations, 1, 5 and 10 mg/ml. Whole blood and colloid samples were mixed in a 1:1 volume ratio, shaken with tapping, and then incubated at 36.5 °C for 30 min and 24 h according to previous report [16,33]. After centrifugation at 3000 rpm for 5 min, the supernatant plasma was removed and let at room temperature during 30 min to allow oxyhemoglobin formation. The absorbance was then measured at 540 nm with a UV/Vis spectrophotometer (SHIMADZU UV-1800). For the estimation of hemolysis percentage, the following equation was used [36]:

$$Hemolysis\% = \frac{(Sample\ absorbance - Negative\ control\ absorbance)}{(Positive\ control\ absorbance - Negative\ control\ absorbance)} \times 100 \quad (1)$$

Three apatite samples prepared on different days were subjected to hemolysis assay to verify reproducibility. Each sample was tested, and all nine test data were utilized to obtain average and standard deviation.

2.4. Interaction with human plasma proteins—protein fluorescence quenching assay

It may be reminded that among most abundant plasma proteins are human serum albumin (~58%), immunoglobulin (~38%) and fibrinogen (~4%). Experiments aiming at investigating interactions between colloidal apatite NPs and plasma proteins were carried out in this work by using individual albumin, fibrinogen and immunoglobulin proteins as well as whole human blood plasma. This study, approved by the Yonsei University Wonju College of Medicine (Approval No. YWMR-12-6-030), was carried out by following the possible quenching of protein fluorescence, which is attributed to the tryptophan residues in protein [37], upon interaction with the NPs via adsorption, agglomeration and/or complexation [38].

Colloids at concentrations of 0, 0.5, 1, 2, 4, 6, 8 and 10 mg/ml were added to plasma (50 times diluted in DPBS) aliquots in a 1:1 volume mixture, and put in a thermos-fine-mixer (FINEPCR SH2000-DX) at 36.5 °C for 30 min with gentle shaking. Luminescence spectrophotometry (Perkin-Elmer LS55, excitation wavelength 280 nm, and emission recorded at 340 nm) was then used on suspension, to determine fluorescence emission intensities. A protein fluorescence quenching ratio was then quantified by the relation:

$$Q = \frac{(I_0 - I)}{I_0} \quad (2)$$

where I_0 and I represent, respectively, fluorescence intensities in the absence and presence of colloids.

Three apatite samples prepared on different days were subjected to fluorescence quenching assay to verify reproducibility of synthesis. Each sample was tested, and all nine test data were utilized to obtain average and standard deviation.

3. Results and discussion

3.1. Physico-chemical characterization of apatite substrate

Figs. 1 and 2 show respectively the XRD and IR patterns of non-colloidal (without dispersing agent) and colloidal particles stabilized by AEP and (PEG)P.

XRD results (Fig. 1) confirm the apatitic nature of the particles as evidenced by comparison with JCPDS file #09-432 relative to stoichiometric hydroxyapatite. However, data analysis points out a lower degree of crystallinity for colloidal samples compared to the non-colloidal reference. This lowered crystallinity has already been discussed previously in the case of AEP-stabilized apatite colloids [29], and was explained by an inhibitory role of AEP blocking some growth surface sites on forming nanocrystals. In the case of

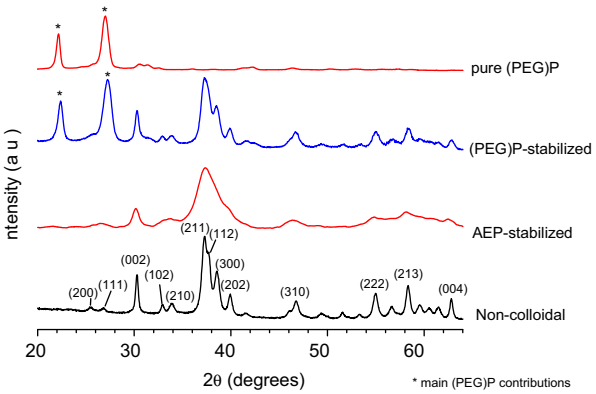

Fig. 1. XRD patterns of biomimetic apatites: AEP- and (PEG)P-stabilized colloids, as well as non-colloidal reference with main indexations after JCPDS file #09-432, and pure (PEG)P.

(PEG)P-stabilized colloids, the crystallinity of the apatite phase is less altered than in the case of AEP. This can be explained by the larger size of the (PEG)P molecule, less prone to hinder apatite crystal growth. The XRD pattern relative to colloidal NPs in the presence of (PEG)P also shows additional broad diffraction lines (especially at 22.4 and 27.3°) which are characteristic of dried (PEG)P. As a control experiment, we also validated by XRD (not shown here for the sake of brevity) that pure (PEG)P did not undergo structural alterations under the conditions used for the preparation of colloids (16 h at 100 °C followed by freeze-drying).

FTIR spectral features (Fig. 2) confirmed XRD conclusions, evidencing vibrations bands characteristic of moderately-well crystallized apatite; a lower resolution was observed for both colloids as compared to the non-colloidal reference sample. The presence of water bands was also revealed, which is customary for biological or biomimetic apatites[39]. Moreover, the stretching vibration mode of apatitic OH^- ions, at 3572 cm^{-1} for hydroxyapatite, as well as the liberation band at 632 cm^{-1}, become less pronounced for the colloids than for the non-colloidal reference, indicating a nonstoichiometry of the apatite phase in presence, as in bone apatite. Additional bands were however also observed in the case of the colloidal NPs, and can be related to the presence of the stabilizing agent. AEP-based apatite colloids displayed in particular a band at 754 cm^{-1}, as previously reported, which is assignable to the P-O-(C) group of AEP molecules in close contact with surface calcium ions[29], as well as vibrational contributions in the region 2900–3400 cm^{-1} related to the ammonium end-group in AEP. In the case of (PEG)P, as can be expected from the long CH_2-CH_2-O carbon chain, numerous additional bands become visible,

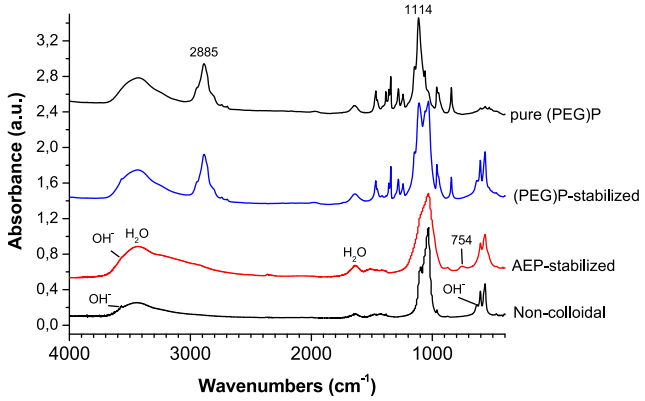

Fig. 2. FTIR spectrum for AEP- and (PEG)P-stabilized colloids, as well as non-colloidal reference and pure (PEG)P.

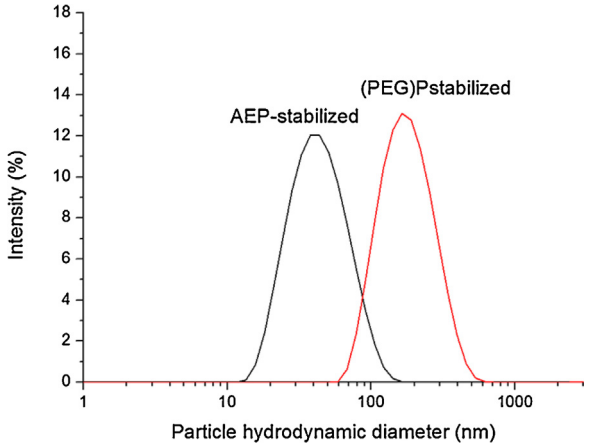

Fig. 3. Particle HD distributions of AEP and (PEG)P colloids as drawn from dynamic light scattering (DLS).

around 2885 cm^{-1} attributable to C-H bonds, and in the region 790–1530 cm^{-1} where multiple contributions arise (C-H, C-C, C-O and P-O), which can be more clearly visualized on the spectrum of pure (PEG)P (Fig. 2). From a chemical viewpoint, the AEP/apatite molar ratio in the nanoparticles of AEP-stabilized colloids is close to 0.7 as estimated from CHN elemental analyses, and the ratio (PEG)P/apatite is estimated to 0.17.

DLS analyses were then carried out to evaluate the particle HD distribution of the colloidal particles obtained. As shown on Fig. 3, the colloid stabilized with AEP was found to be composed of particles exhibiting a monomodal distribution (polydispersity index of 0.163) with a mean HD around 47 nm. This was observed for both the AN and AG variants of this colloid. In contrast, the (PEG)P-stabilized colloids PN and PG were characterized by NPs with mean HDs shifted to larger values, centered around 190 (polydispersity index of 0.151). These results are in good agreement with XRD results which show larger crystal domain size for PN than for AN colloids.

For both colloidal NPs types, zeta potential was also measured, and obtained values are summarized in Table 1. Non-colloidal non-stoichiometric apatite was reported to have a zeta potential value close to −10 mV [29]. As can be seen from this table, there is a significant difference of particles charge between AEP and (PEG)P samples. The smallest nanoparticles are negatively charged, around −48 mV, explained by the addition of a very negative group, HMP. This colloids presents a very electronegative global surface charge, compared to (PEG)P colloids, which zeta potential is close to neutrality (slightly positive).

Table 1
Zeta potential measurements of apatite samples in deionized water and in the presence of plasma: colloidal samples stabilized with AEP (noted A) or with (PEG)P (noted P), either in liquid form (with NaCl, noted N), or freeze-dried (noted G) in the presence of glucose and re-dispersed with NaCl.

Sample ID	Samples only		With plasma	
	pH	Average zeta potential (mV)	pH	Average zeta potential (mV)
AN	6.91	−40 ± 5	7.41	−22 ± 5
AG	7.02	−56 ± 5	7.45	−17 ± 5
PN	7.07	+6 ± 5	7.43	−4.2 ± 5
PG	7.05	+3.5 ± 5	7.35	−6.3 ± 5

3.2. Interaction between Red Blood Cells and nanoparticles—hemolysis evaluation

The investigation of biomimetic colloidal apatite NPs interaction with RBC was carried out here by following the level of hemolysis reached after 30 min or 24 h of contact (see experimental section). Results concerning this hemolytic effect, depending on colloid types and concentrations, are presented in Fig. 4. In the literature, it is customary to consider the value of 5% hemolysis as permissible for biomaterials applications (e.g. Refs. [40–42]). It is apparent from this figure that none of the samples results in serious hemolysis. The level of 5% hemolysis is never reached, except for one type of colloid (AG) and at a very high initial concentration of 10 mg/ml, which is beyond practical value. All other hemolysis rates remain low, although increasing slightly with concentration and time. For AEP-based colloidal suspension AN (not pre-lyophilized), RBC viability is even detected to be (in a reproducible manner) better than for the negative control. This can be explained either by the fact that even during in vitro incubation for negative control, a limited number of cells may however get denatured, and/or by a possible protective effect of this type of colloid. Although AEP liquid (AN) and pre-lyophilized (AG) samples have quite similar physico-chemical properties (HD and zeta potential), they present quite distinct hemolysis rates: AG colloids show somewhat larger RBC degradation, and the difference is accentuated after 24 h. The only differences between these two variants of AEP-stabilized colloid are the presence of glucose for facilitating the freeze-drying/redispersion process and a slightly more negative zeta potential. Several reports have studied the impact of glucose on human RBC membrane, which might indeed explain our present results pointing to a slightly increased degree of hemolysis on glucose-containing formulations: Quan et al. [43] highlighted the cryopreservative effect of some sugar on RBC before freeze-drying, but also some noxious effect. They showed that glucose could induce an elevation of the inner osmorality of RBC leading to osmotic fragility. Schiar et al. [44] also indicated that glucose could increase, although in a limited extent, the toxicity of organic and inorganic compounds and raise hemolysis by maintaining reduced glutathione (GSH) level in erythrocytes. Viskupicova et al. [45] emphasized the role of glucose incubation and concentration dependences on hemolysis; degradative processes increasing with incubation time in the presence of glucose. However, even in the presence of glucose in the AG and PG formulations, no serious hemolysis rate was reached in any case, unless very high concentrations were selected (typically larger than 10 mg/ml) which would be beyond usual practical usage. Considering that hemolysis of NPs are generally carried out in the NP concentration between 0.01 and 2 mg/ml [33,34], the slight toxic effect at 10 mg/ml with current NP is not serious.

Several studies showed that particles surface properties (and in particular surface charge) could affect RBC degradation through direct interaction with erythrocyte membranes. Han et al. [19] studied the interaction between heparin-coated hydroxyapatite nanoparticles and RBC. They demonstrated that their nanoparticles had a strong tendency to favor RBC aggregation, compared to micron-sized particles. They also explained that surface modification of these NPs (initially positively charged) with negative charge through surface immobilization of the drug heparin, could help to limit this cellular aggregation phenomenon, and therefore decrease hemolysis. They concluded that hemocompatibility was rather dependent on particle properties, and especially on surface charge rather than particle size. If we exclude results on the freeze-dried (and re-dispersed) colloids AG and PG, our hemolysis results on AN and PN go also agree with these observations. In the case of the AG and PG formulations, as stated above, the presence of glucose is considered to explain the observed results.

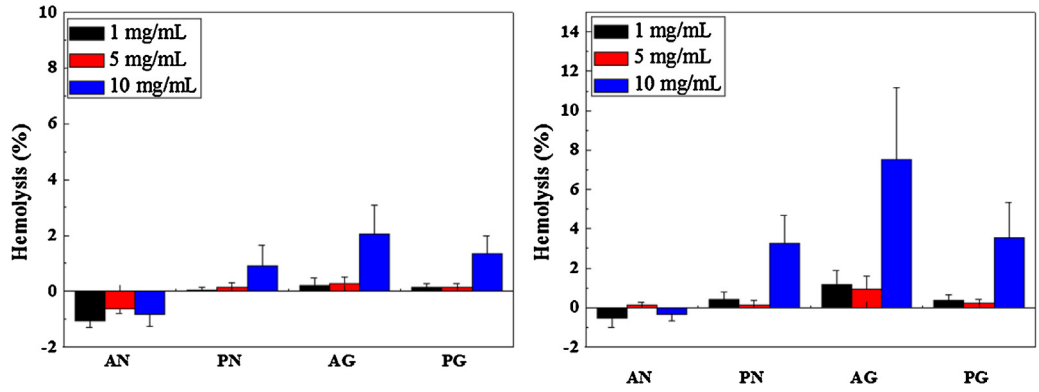

Fig. 4. Hemolytic effect of colloids at 3 different concentrations (initial suspension concentrations: 1, 5 and 10 mg/ml, then mixed in a 1:1 volume ratio with blood), after 30 min and 24 h of incubation.

Globally, this hemolysis study therefore points to a very high hemocompatibility of biomimetic apatite colloidal nanoparticles stabilized by either AEP or (PEG)P as far as the interactions of NPs with RBC go. The next section will then examine the interaction between these NPs with whole human plasma containing in particular another category of blood component: plasmatic proteins.

3.3. Interaction between plasma proteins and nanoparticles—non-specific protein fluorescence quenching study

The level of interaction between plasma proteins and our colloidal NPs is another important aspect to consider for inspecting hemocompatibility [38]. For example, the elimination of pathogens from the body will result in part by the activation of the complement system (a group of plasma proteins active in the immunological body response); and bioavailability of the particles will be altered and probably decreased owing to phagocytosis. It is thus interesting to check if NPs intended for use in contact with blood may or not lead to an important interaction with plasma proteins.

Protein binding was evaluated here, as was done previously [16], by following the degree of fluorescence (through amino acid residues such as tyrosine and tryptophan) of plasma proteins remaining in supernatants after contact with the NPs: a luminescence quenching phenomenon is expected to occur in the case of proteins adsorption on the particles.

Fig. 5 represents the obtained fluorescence quenching ratio as a function of colloids concentrations, both in the case of individual proteins (Fig. 5a) and for while plasma (Fig. 5b). Overall, the tendencies obtained for each triplicate system were found to be very reproducible. All colloids show similar general trends, with increased fluorescence quenching versus NPs concentrations. Results do not change significantly whether individual proteins were considered or while plasma. The AN, PN and PG colloids led to very similar results (up to 0.5–0.7 of quenching ratio), while the AG sample showed even lower quenching effect (~0.3 at 10 mg/ml). It may be remarked for example that these quenching ratios are found to be lower than previously reported values obtained on graphite oxide nanoparticles [16]. In order to inspect more clearly the level of interaction between NPs and plasma proteins, a fitting of the experimental data was then undergone, selecting the date for whole plasma.

Two models were used and compared to analyze the protein binding behavior of our NPs. First Hill equation (also corresponding to Sips or Langmuir-Freundlich isotherm models) was used to describe the fluorescence quenching data, as was done previously on other systems [17]:

Table 2
Analysis of protein fluorescence quenching data: fitted protein-NPs interaction parameters using Hill and Stern-Volmer models.

Hill equation fitted parameters				
	AN	AG	PN	PG
n	0.923	1.17	0.75	0.74
k_D	0.022	0.050	0.0084	0.012
K_b	45.14	19.86	119.5	82.09
r^2	0.970	0.972	0.980	0.992
Stern-Volmer equation fitted parameters				
	AN	AG	PN	PG
k_{sv}	21.01	46.52	99.74	71.15
r^2	0.981	0.991	0.993	0.984

$$\frac{Q}{Q_{\max}} = \frac{[NP]^n}{k_D^n + [NP]^n} \text{Hill equation} \quad (3)$$

where [NP] denotes the concentration of administered NPs, Q is the quenching ratio at concentration [NP], Q_{max} is the maximal quenching ratio of 1, "n" is Hill parameter showing progressive protein binding type on NPs, and k_D is the protein-NP equilibrium constant (at the experimental temperature of 36.5 °C). Hill equation describes here protein-nanoparticles interaction in terms of binding and dissociation. Application of this equation can lead to two major outcomes: Hill parameter "n" and the binding constant "K_b". Cases where $n > 1$ correspond to adsorptive systems with a "positive cooperativity" among adsorbed proteins (proteins affinity to NPs progressively increases), while $n < 1$ indicates that the binding strength of the protein to the NP becomes progressively weaker as further proteins adsorb. The particular case $n = 1$ comes back to an adsorption following a regular Langmuir model. K_b, the protein-NP binding constant, is defined by: $K_b = 1/k_D$.

The second model that was used here to analyze the protein quenching results was Stern-Volmer equation [46]:

$$\frac{I_0}{I} = 1 + k_{sv} \cdot [NP] \text{Stern-Volmer} \quad (4)$$

where [NP] is the concentration of NPs, I_0 the intensity or rate of fluorescence without a quencher, I the intensity or rate of fluorescence with a quencher, and k_{sv} the protein-NP equilibrium constant. This model is generally more suitable for low concentrations (a "domain where quenching is dominated by diffusive transport" [17]); it was considered here for [NP] up to 4 mg/ml. The fitted parameters obtained when applying both models to our data are reported on Table 2.

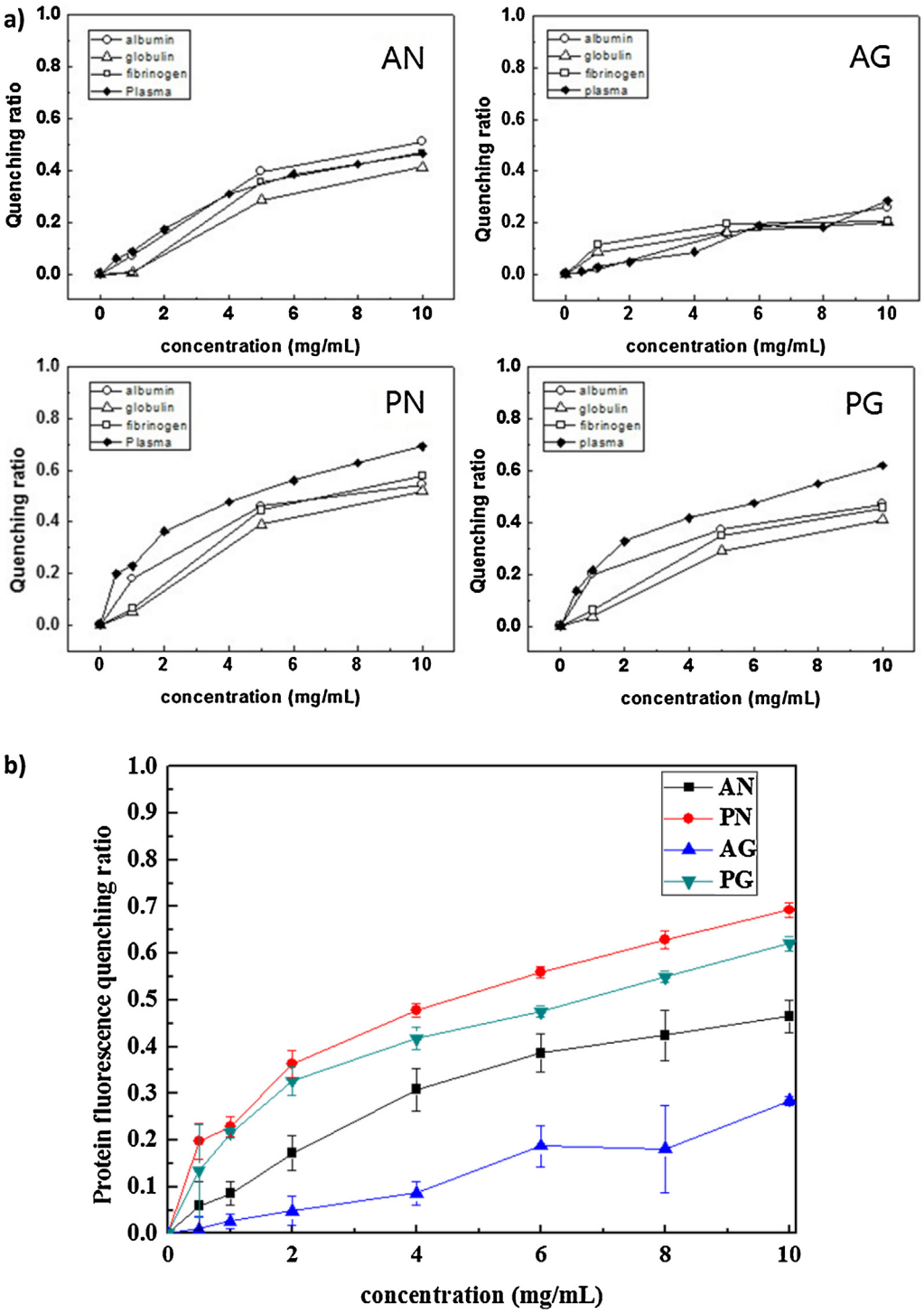

Fig. 5. Fluorescence quenching properties of (a) human serum proteins and full serum (b) summary of data for pure serum, after contact with (PEG)P and AEP colloids.

In each case, correlation coefficients r^2 larger than 0.97 (for Hill plot $r^2 \geq 0.970$, for Stern-Volmer plot $r^2 > 0.98$) were noticed independently of the model (Hill or Stern-Volmer), pointing out the pertinence of these fits. The *n* parameters found with the Hill equation are close to 1 or larger than 1, in the case of AEP colloids, suggesting cooperative adsorption of proteins. In contrast, a value of ~0.75 was observed for (PEG)P. While AEP (and HMP counterions) are small organic molecules with low space occupancy, thus provoking low steric hindrance to protein adsorption, polyethyleneglycol molecules are voluminous; this difference in the size of organic coronas between AEP- and (PEG)P-stabilized colloids could explain the difference in the observed proteins adsorptive behaviors for the two types of colloids.

In terms of binding constants, both models lead to values with an order of magnitude in the range 10^1–10^2 (between 19 and 120 for Hill K_b and between 20 and 100 for Stern-Volmer K_{SV}). Comparatively, significantly larger values were reported in the literature for several other types of nanoparticles (e.g. of the order 10^4–10^7 for citrate-coated gold nanoparticles [17], of the order of 10^3 for graphite oxide nanoparticles [16]). Also, values of the order of 10^4–10^5 were reported for the interaction of flavonoids (a group of polyphenols with potential biomedical applications) with bovine

serum albumin [46]. These findings suggest that the biomimetic apatite-based colloidal nanoparticles tested in this work are fairly inert toward plasma proteins. These results appear all the more appealing that these colloidal biomimetic apatite nanoparticles are fairly inert to plasma proteins thanks to "passive" organic coronas (AEP phospholipid moiety or phosphonated polyethyleneglycol) and do not necessitate additional stabilization via adsorption of a drug such as heparin [19].

Upon treating the samples with blood plasma, it may be noted that DLS measurements led to similar results (within less than 3.5% of difference) before and after plasma contact. In contrast, zeta potential values were significantly modified: highly negative zeta potential of AN and AG shifted to less negative region and positive apatites like PN and PG began to have slightly negative values (see Table 1). These results can be explained by partial protein coverage upon contact with plasma, proteins being known to exhibit negatively-charged residues at physiological pH.

The above discussion thus pointed out the relative inertness of the colloidal NPs tested here with plasma proteins in all cases, which is desirable for usage in nanomedicine. Among the four types of colloids evaluated, some differences of adsorptive behavior can however be distinguished. For any given model, the same general pattern AN < AG < PG < PN is found for interaction constants. Protein-apatite interaction is bound to be greatly governed by NPs characteristics where several parameters may come into play such as surface properties (surface charge, accessibility to surface sites despite organic corona steric hindrance, molecular composition of the corona, specific surface area...) and particle HD. If particle HD was considered alone, AEP colloids (composed of NPs with HD ~ 47 nm) would be expected to have a larger interaction surface and thus to lead to greater interaction with proteins than (PEG)P colloids (NPs ~ 190 nm), especially taking into account the larger space occupancy of polyethyleneglycol. However, this tendency does not fit experimental results (Table 2), indicating that other factors should also be considered, such as surface charge. Indeed, AEP-stabilized colloids are negatively-charged (by way of the HMP treatment) which could explain their lower affinity for proteins (which expose negative end-groups from amino acid residues) compared to the positively-charged (PEG)P-stabilized colloids (PN and PG).

3.4. Concluding remarks

In this contribution, we followed the interaction of two types of biomimetic-apatite colloidal nanoparticles with blood components, namely red blood cells (via hemolysis assays) and plasma proteins (follow-up of non-specific protein adsorption via protein fluorescence quenching).

Hemolysis degrees lower than 5% were observed, pointing out the high hemocompatibility of such colloids with respect to red blood cells. Only one condition (glucose-containing AEP-based freeze-dried colloid) led to a larger level of hemolysis, but this was noticed for high concentration (10 mg/ml) which is beyond expected practical usage, and this result is likely related to the presence of glucose in the formulation. For such colloids, additional research is in progress to select even more suitable soluble matrices for the preparation and re-dispersion of freeze-dried apatite colloids.

In a second stage, the interaction of the NPs with whole human blood plasma as well as with individual proteins was investigated. By following protein luminescence quenching in the presence of the colloids, the extent of NPs/plasma proteins interaction was evaluated experimentally, and the data were then fitted with two models, namely Hill and Stern-Volmer. In all cases and independently of the selected model, interaction constants of the order of 10^1–10^2 were found. These values, significantly lower than those reported for other types of nanoparticles or molecular interactions, indicate the fairly inert character of these colloidal NPs with respect to plasma proteins, again stressing their high hemocompatibility.

It may be noted that, among the four types of colloids (intended for a systemic administration pathway) tested in this study, both hemolysis assays and protein fluorescence quenching data indicated that the AEP-stabilized colloid (not lyophilized) corresponded to the most hemocompatible formulation. It is delicate at this point to determine whether particle size or surface charge is the most relevant factor to take into account in relation with hemocompatibility of such systems. Indeed, both particle size and zeta potential tend to vary simultaneously when changing AEP by (PEG)P. However, it may be concluded from our observations that apatite nanoparticles having initially negative to slightly positive surface charge are compatible to blood components. Also, since the surface charge appears to have eventually a tendency to become slightly negative in all cases after plasma contact, probably due to some extent of protein coverage (partial), then the surface charge parameter is probably less relevant than particle size to distinguish between different categories of apatite colloids, as size remains a characteristic feature of the particles.

This study complements the existing research carried out on biomimetic-apatite-based colloids stabilized by non-drug biocompatible organic molecules. It adds hemocompatibility evidences to the already reported low cytotoxicity and non-pro-inflammatory properties of AEP-stabilized apatite colloids. Future work will aim, among other things, at exploring NPs/cells membranes interactions, and following NPs biodistribution in vivo.

Acknowledgement

The authors wish to thank the CIRIMAT Carnot Institute for financing of M. Choimet's PhD thesis grant.

References

[1] A. Bouladjine, A. Al-Kattan, P. Dufour, C. Drouet, New advances in nanocrystalline apatite colloids intended for cellular drug delivery, Langmuir 25 (2009) 12256–12265, http://dx.doi.org/10.1021/la901671j.
[2] D. Chen, Z. Luo, N. Li, J.Y. Lee, J. Xie, J. Lu, Amphiphilic polymeric nanocarriers with luminescent gold nanoclusters for concurrent bioimaging and controlled drug release, Adv. Funct. Mater. 23 (2013) 4324–4331, http://dx.doi.org/10.1002/adfm.201300411.
[3] S. Ferber, H. Baabur-Cohen, R. Blau, Y. Epshtein, E. Kisin-Finfer, O. Redy, et al., Polymeric nanotheranostics for real-time non-invasive optical imaging of breast cancer progression and drug release, Cancer Lett. 352 (2014) 81–89, http://dx.doi.org/10.1016/j.canlet.2014.02.022.
[4] D.F. Emerich, C.G. Thanos, The pinpoint promise of nanoparticle-based drug delivery and molecular diagnosis, Biomol. Eng. 23 (2006) 171–184, http://dx.doi.org/10.1016/j.bioeng.2006.05.026.
[5] J.E. Schroeder, I. Shweky, H. Shmeeda, U. Banin, A. Gabizon, Folate-mediated tumor cell uptake of quantum dots entrapped in lipid nanoparticles, J. Control. Release 124 (2007) 28–34, http://dx.doi.org/10.1016/j.jconrel.2007.08.028.
[6] A. Al-Kattan, S. Girod-Fullana, C. Charvillat, H. Ternet-Fontebasso, P. Dufour, J. Dexpert-Ghys, et al., Biomimetic nanocrystalline apatites: emerging perspectives in cancer diagnosis and treatment, Int. J. Pharm. 423 (2012) 26–36, http://dx.doi.org/10.1016/j.ijpharm.2011.07.005.
[7] K.Y. Choi, G. Liu, S. Lee, X. Chen, Theranostic nanoplatforms for simultaneous cancer imaging and therapy: current approaches and future perspectives, Nanoscale 4 (2012) 330–342, http://dx.doi.org/10.1039/c1nr11277e.
[8] M.S. Murahari, M.C. Yergeri, Identification and usage of fluorescent probes as nanoparticle contrast agents in detecting cancer, Curr. Pharm. Des. 19 (2013) 4622–4640.
[9] M. Iafisco, J.M. Delgado-Lopez, E.M. Varoni, A. Tampieri, L. Rimondini, J. Gomez-Morales, et al., Cell surface receptor targeted biomimetic apatite nanocrystals for cancer therapy, Small 9 (2013) 3834–3844, http://dx.doi.org/10.1002/smll.201202843.
[10] F. Oltolina, L. Gregoletto, Monoclonal antibody-targeted fluorescein-5-isothiocyanate-labeled biomimetic nanoapatites: a promising fluorescent probe for imaging applications, Langmuir (2015) 1–6, http://dx.doi.org/10.1021/la503747s.
[11] B. Sandhöfer, M. Meckel, J.M. Delgado-López, T. Patrício, A. Tampieri, F. Rösch, et al., Synthesis and preliminary in vivo evaluation of well-dispersed biomimetic nanocrystalline apatites labeled with positron emission

tomographic imaging agents, ACS Appl Mater. Interfaces 7 (2015) 10623–10633, http://dx.doi.org/10.1021/acsami.5b02624.
[12] M.A. Dobrovolskaia, P. Aggarwal, J.B. Hall, S.E. McNeil, Preclinical studies to understand nanoparticle interaction with the immune system and its potential effects on nanoparticle biodistribution, Mol. Pharm. 5 (2008) 487–495, http://dx.doi.org/10.1021/mp800032f.
[13] N.R. Kuznetsova, C. Sevrin, D. Lespineux, N.V. Bovin, E.L. Vodovozova, T. Mészáros, et al., Hemocompatibility of liposomes loaded with lipophilic prodrugs of methotrexate and melphalan in the lipid bilayer, J. Control. Release 160 (2012) 394–400, http://dx.doi.org/10.1016/j.jconrel.2011.12.010.
[14] A. Yildirim, E. Ozgur, M. Bayindir, Impact of mesoporous silica nanoparticle surface functionality on hemolytic activity, thrombogenicity and non-specific protein adsorption, J. Mater. Chem. B 1 (2013) 1909, http://dx.doi.org/10.1039/c3tb20139b.
[15] C. Fornaguera, G. Calderó, M. Mitjans, M.P. Vinardell, C. Solans, C. Vauthier, Interactions of PLGA nanoparticles with blood components: protein adsorption, coagulation, activation of the complement system and hemolysis studies, Nanoscale 7 (2015) 6045–6058, http://dx.doi.org/10.1039/C5NR00733J.
[16] H.-M. Kim, K.-M. Kim, K. Lee, Y.S. Kim, J.-M. Oh, Nano-bio interaction between graphite oxide nanoparticles and human blood components, Eur. J. Inorg. Chem. 2012 (2012) 5343–5349, http://dx.doi.org/10.1002/ejic.201200587.
[17] S.H.D.P. Lacerda, J.J. Park, C. Meuse, D. Pristinski, M.L. Becker, A. Karim, et al., Interaction of gold nanoparticles with common human blood proteins, ACS Nano 4 (2010) 365–379, http://dx.doi.org/10.1021/nn9011187.
[18] A. Mayer, M. Vadon, B. Rinner, A. Novak, R. Wintersteiger, E. Fröhlich, The role of nanoparticle size in hemocompatibility, Toxicology 258 (2009) 139–147, http://dx.doi.org/10.1016/j.tox.2009.01.015.
[19] Y. Han, X. Wang, H. Dai, S. Li, Nanosize and surface charge effects of hydroxyapatite nanoparticles on red blood cell suspensions, ACS Appl. Mater. Interfaces 4 (2012) 4616–4622, http://dx.doi.org/10.1021/am300992x.
[20] T. Welzel, I. Radtke, W. Meyer-Zaika, R. Heumann, M. Epple, Transfection of cells with custom-made calcium phosphate nanoparticles coated with DNA, J. Mater. Chem. 14 (2004) 2213, http://dx.doi.org/10.1039/b401644k.
[21] A. Al-Kattan, P. Dufour, J. Dexpert-Ghys, C. Drouet, Preparation and physicochemical characteristics of luminescent apatite-Based colloids, J. Phys. Chem. C 114 (2010) 2918–2924, http://dx.doi.org/10.1021/jp910923g.
[22] C. Drouet, A. Al-Kattan, M. Choimet, A. Tourrette, V. Santran, J. Dexpert-Ghys, et al., Biomimetic apatite-based functional nanoparticles as promising newcomers in nanomedicine: overview of 10 years of initiatory research, J. Gen. Pract. Med. Diagnosis (2015), http://oatao.univ-toulouse.fr/14233/1/drouet_14233.pdf (accessed 10.09.15).
[23] M. Tourbin, A. Al-Kattan, C. Drouet, Study on the stability of suspensions based on biomimetic apatites aimed at biomedical applications, Powder Technol. 255 (2014) 17–22, http://dx.doi.org/10.1016/j.powtec.2013.08.008.
[24] V. Sarath Chandra, G. Baskar, R.V. Suganthi, K. Elayaraja, M.I. Ahymah Joshy, W. Sofi Beaula, et al., Blood compatibility of iron-doped nanosize hydroxyapatite and its drug release, ACS Appl. Mater. Interfaces 4 (2012) 1200–1210, http://dx.doi.org/10.1021/am300140q.
[25] E.M. Múzquiz-Ramos, D.A. Cortés-Hernández, J.C. Escobedo-Bocardo, A. Zugasti-Cruz, X.S. Ramírez-Gómez, J.G. Osuna-Alarcón, In vitro and in vivo biocompatibility of apatite-coated magnetite nanoparticles for cancer therapy, J. Mater. Sci. Mater. Med. 24 (2013) 1035–1041, http://dx.doi.org/10.1007/s10856-013-4862-0.
[26] A. Ashokan, G.S. Gowd, V.H. Somasundaram, A. Bhupathi, R. Peethambaran, A.K.K. Unni, et al., Multifunctional calcium phosphate nano-contrast agent for combined nuclear, magnetic and near-infrared in vivo imaging, Biomaterials 34 (2013) 7143–7157, http://dx.doi.org/10.1016/j.biomaterials.2013.05.077.
[27] W.S. Vedakumari, V.M. Priya, T.P. Sastry, Deposition of superparamagnetic nanohydroxyapatite on iron–fibrin substrates: preparation, characterization, cytocompatibility and bioactivity studies, Colloids Surf. B: Biointerfaces 120 (2014) 208–214, http://dx.doi.org/10.1016/j.colsurfb.2014.04.021.
[28] L. Montazeri, J. Javadpour, M.A. Shokrgozar, S. Bonakdar, M. Khayyat Moghaddam, V. Asgary, The interaction of plasma proteins with nano-size fluoride-substituted apatite powders, Ceram. Int. 39 (2013) 6145–6152, http://dx.doi.org/10.1016/j.ceramint.2013.01.033.
[29] A. Al-Kattan, V. Santran, P. Dufour, J. Dexpert-Ghys, C. Drouet, Novel contributions on luminescent apatite-based colloids intended for medical imaging, J. Biomater. Appl. 28 (2014) 697–707 http://www.ncbi.nlm.nih.gov/pubmed/23418200.
[30] L. Rothfield, A. Finkelstein, Membrane biochemistry, Annu. Rev. Biochem. 37 (1968) 463–496, http://dx.doi.org/10.1146/annurev.bi.37.070168.002335.
[31] J. Gómez-Morales, M. Iafisco, J.M. Delgado-López, S. Sarda, C. Drouet, Progress on the preparation of nanocrystalline apatites and surface characterization: overview of fundamental and applied aspects, Prog. Cryst. Growth Charact. Mater. 59 (2013) 1–46, http://dx.doi.org/10.1016/j.pcrysgrow.2012.11.001.
[32] A. Al-Kattan, P. Dufour, C. Drouet, Purification of biomimetic apatite-based hybrid colloids intended for biomedical applications: a dialysis study, Colloids Surf. B: Biointerfaces 82 (2011) 378–384, http://dx.doi.org/10.1016/j.colsurfb.2010.09.022.
[33] Y.-S. Lin, C.L. Haynes, Impacts of mesoporous silica nanoparticle size, pore ordering, and pore integrity on hemolytic activity, J. Am. Chem. Soc. 132 (2010) 4834–4842, http://dx.doi.org/10.1021/ja910846q.
[34] J. Choi, V. Reipa, V.M. Hitchins, P.L. Goering, R.A. Malinauskas, Physicochemical characterization and in vitro hemolysis evaluation of silver nanoparticles, Toxicol. Sci. 123 (2011) 133–143, http://dx.doi.org/10.1093/toxsci/kfr149.
[35] T. Yu, A. Malugin, H. Ghandehari, Impact of silica nanoparticle design on cellular toxicity and hemolytic activity, ACS Nano 5 (2011) 5717–5728, http://dx.doi.org/10.1021/nn2013904.
[36] J. Autian, Biological model systems for the testing of the toxicity of biomaterials, in: P. Press (Ed.), Polym. Med. Surg., vol. 8, Springer Science & Business Media, New York, 1996, p. 181.
[37] L. Lai, C. Lin, Z.-Q. Xu, X.-L. Han, F.-F. Tian, P. Mei, et al., Spectroscopic studies on the interactions between CdTe quantum dots coated with different ligands and human serum albumin, Spectrochim. Acta. A: Mol. Biomol. Spectrosc. 97 (2012) 366–376, http://dx.doi.org/10.1016/j.saa.2012.06.025.
[38] P. Aggarwal, J.B. Hall, C.B. McLeland, M.A. Dobrovolskaia, S.E. McNeil, Nanoparticle interaction with plasma proteins as it relates to particle biodistribution, biocompatibility and therapeutic efficacy, Adv. Drug Deliv. Rev. 61 (2009) 428–437, http://dx.doi.org/10.1016/j.addr.2009.03.009.
[39] N. Vandecandelaere, C. Rey, C. Drouet, Biomimetic apatite-based biomaterials: on the critical impact of synthesis and post-synthesis parameters, J. Mater. Sci. Mater. Med. 23 (2012) 2593–2606, http://dx.doi.org/10.1007/s10856-012-4719-y.
[40] Q.Z. Wang, X.G. Chen, Z.X. Li, S. Wang, C.S. Liu, X.H. Meng, et al., Preparation and blood coagulation evaluation of chitosan microspheres, J. Mater. Sci. Mater. Med. 19 (2008) 1371–1377, http://dx.doi.org/10.1007/s10856-007-3243-y.
[41] H. Hu, X.B. Wang, S.L. Xu, W.T. Yang, F.J. Xu, J. Shen, et al., Preparation and evaluation of well-defined hemocompatible layered double hydroxide-poly(sulfobetaine) nanohybrids, J. Mater. Chem. 22 (2012) 15362, http://dx.doi.org/10.1039/c2jm32720a.
[42] C. Hou, Q. Yuan, D. Huo, S. Zheng, D. Zhan, Investigation on clotting and hemolysis characteristics of heparin-immobilized polyether sulfones biomembrane, J. Biomed. Mater. Res. A 85 (2008) 847–852, http://dx.doi.org/10.1002/jbm.a.31502.
[43] G.B. Quan, Y. Han, M.X. Liu, L. Fang, W. Du, S.P. Ren, et al., Addition of oligosaccharide decreases the freezing lesions on human red blood cell membrane in the presence of dextran and glucose, Cryobiology 62 (2011) 135–144, http://dx.doi.org/10.1016/j.cryobiol.2011.01.015.
[44] V.P.P. Schiar, D.B. Dos Santos, M.W. Paixão, C.W. Nogueira, J.B.T. Rocha, G. Zeni, Human erythrocyte hemolysis induced by selenium and tellurium compounds increased by GSH or glucose: a possible involvement of reactive oxygen species, Chem. Biol. Interact. 177 (2009) 28–33, http://dx.doi.org/10.1016/j.cbi.2008.10.007.
[45] J. Viskupicova, D. Blaskovic, S. Galiniak, M. Soszyński, G. Bartosz, L. Horakova, et al., Effect of high glucose concentrations on human erythrocytes in vitro, Redox Biol. 5 (2015) 381–387, http://dx.doi.org/10.1016/j.redox.2015.06.011.
[46] A. Papadopoulou, R.J. Green, R.A. Frazier, Interaction of flavonoids with bovine serum albumin: a fluorescence quenching study, J. Agric. Food Chem. 53 (2005) 158–163, http://dx.doi.org/10.1021/jf048693g.